

7/13/98

Icarus revisited:
Three decades of radar observation of asteroids

Pravas R. Mahapatra*
Steven J. Ostro
Lance A. M. Benner
Keith D. Rosema
Raymond F. Jurgens
Ron Winkler
Randy Rose
Jon D. Giorgini
Donald K. Yeomans
Martin A. Slade

All authors are with:

Jet Propulsion Laboratory
California Institute of Technology
4800 Oak Grove Drive
Pasadena, CA 91109-8099
U.S.A.

Corresponding Author:
(for sending proofs and offprint requests)

Dr. Steven J. Ostro
300-233
Jet Propulsion Laboratory
4800 Oak Grove Drive
Pasadena, CA 91109-8099
U.S.A.

Phone: 818-354-3173
Fax: 818-354-9476
E-mail: ostro@echo.jpl.nasa.gov

*On leave from Indian Institute of Science, Bangalore 560012, India.

Abstract. Three decades after the close encounter of 1566 Icarus, which marked the beginning of asteroid radar astronomy, we had a chance to observe the asteroid afresh by using a more developed radar system, and here we present the results of that study. Some of the original conclusions made by the pioneering observers appear to be essentially well-founded. However, the radar cross section of the asteroid is found to be only about a half of the earlier estimates. Doppler analysis shows the possibility of the body being somewhat smaller than hitherto thought, with the lower bound on the size of Icarus being in the range of 0.57-0.77 km. The radar albedo of 10-17% that we estimate is not contrary to Icarus' tentative classification as an S-type object. Further, Icarus is found to induce a polarization ratio between about 0.3 and 0.7 at X-band ($\lambda = 3.5$ cm), signifying a rough surface in the centimeter-to-decimeter scale.

Introduction

The Apollo asteroid 1566 Icarus was discovered by W. Baade at the Palomar observatory on 27 June 1949. The radar observation of this body during a close apparition in 1968 marked the beginning of asteroid radar astronomy. The encounter had caused considerable concern to the world community because of a suspected collision probability (Nature, 1967; Newsweek, 1968), triggered discussions on ways to counter such collisions (Kleiman, 1968), and led to serious pleas for monitoring asteroids and exploring them by spacecraft (New York Times, 1967; 1968; 1969). A large number of articles were published on the topic during 1967-70 (<http://pdssbn.astro.umd.edu/SBNast/archive/refs.tab>). Table I lists some of the news items and popular and semipopular articles of the time, indicating the extraordinary level of social interest aroused by Icarus' close encounter.

Icarus has several noteworthy features. It is among the fastest rotators¹ and the closest to approach the sun². The latter property, together with its high orbital eccentricity, make Icarus a more attractive object than Mercury for testing gravitational theories (Shahid-Salass and Yeomans, 1994). The same orbital parameters have led to speculation that the object may be a spent comet. Icarus is also believed to be one of the most spheroidal near-earth asteroids (NEAs) (McFadden *et al.*, 1989), which are generally irregular in shape with high aspect ratios, presumably because of their collisional origin. Its shape has been estimated to be within 5% of a sphere by Miner and Young (1969), and within 10% by Gehrels *et al.* (1970).

¹Only two asteroids are known to date that spin faster than Icarus: 1995 HM with a period of 1.62 h (Steel *et al.*, 1997), and the just-discovered (May 1998) 1998 KY26 which appears to have a spin period of the order of 11 minutes.

²Two known asteroids with shorter perihelion q are 3200 Phaethon ($q = 0.14$ AU) and 1995 CR ($q = 0.12$ AU).

During an apparition in 1996 we had a chance to observe Icarus using an improved radar system. This paper presents the results of that study and, while putting them in perspective with the pioneering observations of 1968, touches upon some of the intervening developments.

Non-Radar Data

As an asteroid of relatively long observational history, Icarus' ephemeris has been established with very high precision, but the same is not true of the size and physical characteristics of the body. As shown in Table II, estimates of its visual magnitude vary almost by a magnitude. The taxonomic classification of Icarus is also uncertain. The authoritative works of Tholen (1989) and McFadden *et al.* (1989, Table I) do not assign a class to this object, while other studies assign it an S or Q class (Table II).

There also exists uncertainty regarding the asteroid's size. In the absence of opportunities for direct occultation, optical assessment of its size has been based on indirect methods. Comprehensive tables of asteroid properties such as that of Tedesco (1989) do not quote a diameter. Gehrels *et al.* (1970) estimated Icarus' diameter as 0.54 km, which agreed quite well with radar estimates of the object's size, which we discuss below.

The First Radar View of Icarus

8

The 1968 apparition of Icarus (0.043 AU at its closest) was observed by Goldstein (1968, 1969) with the Goldstone radar at a continuous-wave (CW) frequency of 2388 MHz, and by Pettengill *et al.* (1969) at 7840 MHz with the Haystack radar. Goldstein (1968) derived a radar cross section (RCS) of 0.1 km² for Icarus and constrained its radius and rotation period to be 0.3–0.6 km and 1.5–3.3 h respectively. Subsequently the precise spin rate and axis orientation of Icarus became available through light-curve studies by Gehrels *et al.* (1970). Using these results (prior to their publication), Goldstein (1969) refined his radius estimate to be ≥ 490 m, and constrained the reflectivity to be ≤ 0.13 .

Goldstein (1968) had reported a splitting of the spectral peak from a unimodal shape to a bimodal one as the spectrum evolved during June 14–16, 1968, but Pettengill *et al.* (1969) did not notice any spectral splitting. They proposed an RCS of ~ 0.1 km², radius of ~ 1 km, and effective reflectivity of ~ 0.05 as the most likely parameters for Icarus within a possible uncertainty factor of 2.

Intervening Developments

Since the first experiments in radar echoing of an asteroid, numerous developments have occurred in the

related disciplines. Upgrades of astronomical radars at Goldstone and Arecibo have included transmitter power enhancement, improvements of the antenna and feed structures, and, in the case of the latter, incorporation of ground interference screening structures. Importantly, they have been provided with simultaneous dual polarization reception capability, adding a new dimension of information to astronomical observations.

This period has also seen rapid technological development in the areas of data handling, reduction, processing, storage, and display. Automated radar operation and real-time signal and data processing enables more efficient utilization of the limited windows of opportunity for asteroid observation. It is now possible to perform multi-parameter (Range-Doppler-Polarization) observation and processing of asteroid signals, under favorable conditions, to constrain asteroid shapes and surface features (e.g. Ostro *et al.*, 1995).

Significant advance has also been made in the knowledge base of asteroid radar signatures and their interpretation, with 37 MBAs (main-belt asteroids) and 48 NEAs observed by July 1998. The interpretation of these radar data, by themselves and together with optical and infrared data, have generated a fair degree of understanding regarding the behavior of asteroids of different classes as radar targets, and augmented the basic understanding of these bodies (e.g. Ostro *et al.*, 1991a).

In the period since its first detection in 1968, Icarus presented one more window of potential opportunity for radar observation during 20-22 June, 1987 when it came within 0.16 AU from the Earth. It had the right geometrical visibility parameters for observation by the Arecibo astronomical radar. Yet, contrary to expectation based on earlier RCS data, no detection was achieved. This gave the first indication that the actual RCS of Icarus may be lower than 0.1 km².

A Recent Radar View of Icarus

Data Collection and Integration

The present study is based on data collected by the JPL's Goldstone radar through its 70-meter DSS-14 antenna during an apparition of Icarus lasting through 8-12 June 1996. As the echoes were expected to be weak, only CW data were collected for the first three days. The parameters of data collection are listed in Table III. Each data run comprised the echo samples obtained over a time period slightly less than the round-trip light time in response to a transmission of the same length. Attempts to obtain range-Doppler echoes on June 11 and 12 using phase-coded transmission were unsuccessful.

The signal-to-noise ratios (SNRs) of the single-run spectra were very weak. Summation over all the runs in each day made the target detectable, but the SNR was still inadequate to make reliable quantitative deductions. We therefore performed a higher level of integration by summing the spectra across all the three days. The data covered multiple rotations of Icarus (Fig. 1), so such integration entails a loss of rotational resolution.

Heuristic Analysis

We first perform a simple visual analysis of the Doppler data as was done by the pioneering radar observers of Icarus in 1968. The raw 3-day weighted sum spectrum is shown in Fig. 2a. As this spectrum is too jagged (peak SNR ~ 3), it is smoothed with a 10-Hz filter (Fig. 2b), yielding SNR ~ 7 . To enhance the SNR even further, we fold the Doppler spectrum about the DC line, (i.e. invert the spectrum of Fig. 2b about the zero-Doppler axis and add it to the uninverted spectrum). Such an operation is admissible if the echo's center-of-mass frequency offset is small compared to the spectral resolution, which is the case here. For Icarus, analysis of all available optical and radar astrometry (http://ssd.jpl.nasa.gov/radar_data.html) yields an orbit (<http://ssd.jpl.nasa.gov/cgi-bin/eph>) which predicts that the correction to the Goldstone Doppler ephemeris was 0.65 Hz, i.e. 1/3 of our raw spectral resolution. The folded spectrum, which has SNR close to 10, is shown in Fig. 2c. Its central portion is expanded in Fig. 2d, which indicates an extremal (edge-to-edge) or zero-crossing bandwidth B of about 45 Hz for the OC spectrum. Since the 10-Hz smoothing would have stretched the bandwidth by about the same amount, the actual value of B is likely to be about 35 Hz. There would also be a small bias in the bandwidth estimate due to the FFT resolution of 1.95 Hz which is neglected. Using the equation

$$B(\delta) \leq \frac{4\pi D \cos \delta}{\lambda P} \quad (1)$$

where D is the "effective" equatorial diameter of the asteroid³, δ is the angle between the radar-asteroid line and the equatorial plane of the asteroid, λ is the radar wavelength, and P is the apparent rotation period of

³When Eq. (1) is applied to the instantaneous bandwidth of the echo spectrum, D is the breadth of the plane-of-sky projection of the asteroid's pole-on silhouette. However, in a case like the current one, where the spectrum has been integrated over more than one full rotation of the body which is quasi-spherical, the dimension D would be expected to be equal to, or perhaps slightly greater than, the maximum pole-on breadth.

the asteroid, a 35 Hz bandwidth corresponds to $D \geq 0.8$ km.

Formal Analysis

We now make a formal analysis that is more robust against noise effects, and explicitly takes into account the radar scattering behavior of Icarus. This is done by least-squares-fitting the unimodal function⁴

$$y(f) = a \left[1 - \left(\frac{f - d_{off}}{B/2} \right)^2 \right]^{\frac{n}{2}} \quad (2)$$

to the raw spectrum, where a is the amplitude of the model function, f is the Doppler frequency, d_{off} is the offset of the center frequency of the target spectrum with respect to the Doppler-prediction ephemeris, and n is a shape parameter. In general n depends on the radar backscattering behavior of the asteroid surface with respect to the angle of incidence, the shape of the object, and the reflectivity or ‘feature’ distribution on its surface. However, in the present case, with a quasi-spherical shape of the asteroid and data integration over many rotations, the spectrum shape parameter n in Eq. (2) is expected to be predominantly dependent on the average surface backscattering property of the asteroid.

Figure 3 shows the χ^2 values for the best-fitting model curve over a range of B and n values. A clear minimum exists for any given value of n or B , but the surface has a diagonal trough which yields a coupled constraint for B (and hence D) and n which cannot be resolved by the OC spectrum alone. However, the differential polarization behavior of the asteroid surface can help in this respect. As seen from Fig. 2a, the power in the OC and SC spectra vary with a certain degree of independence over the spectral domain, and their ratio μ_c is a function of the particular frequency band chosen.

Table IV shows that μ_c varies between 0.38 and 0.76 over the bandwidth of our interest. These high values point to the existence of considerable surface roughness at spatial scales of the order of λ . One would thus be justified in assuming a fairly diffuse surface for Icarus, possibly with n in the range of 3–5. The corresponding B from Fig. 3 would lie between 25 and 35 Hz, with Eq. (1) yielding a lower bound for D between 0.57 and 0.77 km based on a quasi-spherical assumption. These are less than the original estimates made by both Goldstein (1969) and Pettengill *et al.* (1969). Note here that a ~ 1 km diameter, as currently believed, plus the assumption of a nearly equatorial view, would lead to $B \approx 45$ Hz, for which $n > 10$ (Fig.

⁴The function (2) corresponds to the Doppler spectral shape of the echo signals from a rotating spherical object of uniform surface scattering property modeled as $\cos^n \theta$ where θ is the angle from the incidence direction.

4), and μ_c would be 0.69. Such a combination is not normally considered mutually compatible.

Radar Cross Section and Albedo

The OC RCS σ_{OC} of Icarus lies between 0.046 and 0.054 km² for B in the range of 25–35 Hz (Table IV). Given the expected uncertainties in absolute echo power estimates by the Goldstone radar, we adopt the mean value of 0.05 km² as the σ_{OC} estimate (with an uncertainty in the region of 35%), which is only about a half of the RCS estimated by Goldstein (1968,1969). Noting that we also observed from Doppler analysis a smaller lower bound for D than earlier estimates, a lower σ_{OC} appears plausible.

For each assumed B , the radar albedo $\hat{\sigma}_{OC}$ of Icarus has been calculated using $\sigma_{OC} = 0.05$ km² and a spherical projected area with D equal to the bound obtained from Eq. (1). In Table IV, for the B interval of 25–35 Hz, $\hat{\sigma}_{OC}$ varies from about 0.17 to 0.10, which is in general agreement with $\hat{\sigma}_{OC} \leq 0.13$ as determined by Goldstein (1969). Such agreement, however, is the result of our estimates of both σ_{OC} and D being smaller than his by about the same factor. Further, observing that the average $\hat{\sigma}_{OC}$ of S-class NEAs is estimated at between 0.15 and 0.16 (Ostro *et al.*, 1991a, and including subsequently observed NEA radar albedos), our $\hat{\sigma}_{OC}$ estimate of Icarus does not contradict its classification as an S-type object, though the observed albedo alone cannot be taken as confirmation of such classification.

Correlation with Visual Albedo

Figure 4 shows a plot of $\hat{\sigma}_{OC} = \sigma_{OC}/(\pi D^2/4)$ with $\sigma_{OC} = 0.05$ km², and depicts the variation of the visual geometric albedo p_v corresponding to the two extremes of the absolute magnitude H quoted for Icarus (Table II). p_v is obtained from the relation (Zellner, 1979)

$$\log p_v = 6.244 - 2 \log D - 0.4H. \quad (3)$$

Also marked on the $\hat{\sigma}_{OC}$ - D curves in Fig. 4 are the points whose ordinates correspond to the average radar albedo of NEAs and MBAs by taxonomic class. The interval of 0.57–0.77 km, where we place the upper bound of Icarus' diameter, is seen to fall in the middle of the known asteroid $\hat{\sigma}_{OC}$ distribution.

Considering the p_v curve for $H = 15.95$, $D = 0.9$ km would lead to a very high p_v of ~ 0.95 , and the D interval of 0.57–0.77 km would yield $p_v > 1$. The p_v values are more realistic (38% for 0.9 km, 51–94% for 0.57–0.77 km) if $H = 16.9$. Thus, if Icarus has a diffuse surface and if its view was near-equatorial, then its magnitude would be closer to (or perhaps numerically greater than) 16.9 than 15.95. Even $D = 0.9$ km

favors the former absolute magnitude than the latter.

Polarization Behavior

In the B interval of 25–35 Hz, μ_c is observed from Table IV to be between 0.44 and 0.52. Even after accounting for the estimation uncertainty of 12–13%, these values are considered high for asteroids in general and NEAs in particular (Ostro, 1993), but are not unique. Two other NEAs exhibiting such high circular polarization ratios at $\lambda = 3.5$ cm are 1981 Midas ($\mu_c \sim 0.65$) and 3908 (1980 PA) ($\mu_c \sim 0.72$) (Ostro *et al.*, 1991b). Further, the asteroids 2101 Adonis, 3103 Eger, and 1992 QN have recently been found to have near-unity circular polarization ratios (Benner *et al.*, 1997). High polarization ratios are often associated with surface regoliths. In the case of Icarus, its small size and rapid rotation would argue against its ability to hold loose surface regolith. However, McFadden *et al.* (1989) are of the opinion that several NEAs do support regoliths (perhaps dusty), and that “the controlling factors of regolith properties and processes are not simply due to scaling with size and gravity.” Since the X-band of radar frequencies require roughness only of the order of centimeters to tens of centimeters to produce significant depolarization, the observation in the case of Icarus could possibly also be explained by surface granularity resulting from fracture along grain boundaries of crystalline, layered, or nodular rocky material in a parent body. This hypothesis would, of course, assume the asteroid to be of recent origin, without having undergone smoothing due to micrometeoritic ‘weathering’. The possibility for high polarization ratios involving volume scattering within icy media appear remote in the case of Icarus because of the absence of coma at its close perihelion.

Concluding Remarks.

Based on fresh radar observations of 1566 Icarus during a recent apparition, some of the major parameters of the asteroid have been estimated and compared with those derived during the pioneering observations that ushered in the era of asteroid radar astronomy three decades ago. The recent observations are not seriously inconsistent with the findings of the first study, and bear testimony to the ability of the pioneers in deducing meaningful data from very limited observations. However, it is found that the lower limit of 0.98 km set on the diameter earlier may not be a hard one, and that there is a distinct possibility of Icarus being as small as a little over one-half of a kilometer across.

It is in order to point out here that the basic signal quality (as expressed by SNR) received during the recent experiments was not substantially better than the first observation in 1968. This comparison must

be made in the background of the great difference in the range of the asteroid during the two approaches. The object was farther from the Earth in 1996 than in 1968 by a factor of 2.4 which, by the inverse-fourth-power dependence of radar return on range, should yield an echo power over 30 times weaker if all other parameters remain invariant. It is due to the advances in the radar capabilities during the intervening decades that windows of opportunity for astrometric observation have been considerably broadened.

The next radar opportunity to observe Icarus will arise in June 2015 when the asteroid will pass within 0.054 AU of the Earth. This is just over half the distance of the 1996 apparition studied here, and this fact alone should provide an SNR 12 times larger. Any improvement in radar sensitivity by that time would further enhance Icarus' radar observability, and provide a much more detailed picture of the object.

ACKNOWLEDGMENTS

Pravas R. Mahapatra and Lance M. Benner were supported as Research Associates of the National Research Council. Part of this research was conducted at the Jet Propulsion Laboratory, California Institute of Technology, under contract with the National Aeronautics and Space Administration (NASA).

REFERENCES

- Benner, L. A. M., Ostro, S. J., Giorgini, J. D., Jurgens, R. F., Mitchell, D. L., Rose, R., Rosema, K. D., Slade, M. A., Winkler, R. and Yeomans, D. K. (1997) Radar detection of near-Earth asteroids 2062 Aten, 2101 Adonis, 3103 Eger, 4544 Xanthus, and 1992 QN. *Icarus* **130**, 296-312.
- Chapman, C. R., Morrison, D. and Zellner, B. (1975) Surface properties of asteroids: A synthesis of polarimetry, radiometry, and spectrophotometry. *Icarus* **25**, 104-130.
- Chapman, C. R., Harris, A. W. and Binzel, R. (1994) Physical properties of near-earth asteroids: implications for the hazard issue. In *Hazards due to Comets and Asteroids*, ed. T. Gehrels, pp. 537-549. Univ. of Arizona Press, Tucson.
- Gehrels, T., Roemer, E., Taylor, R. C., and Zellner, B. H. (1970) Minor planets and related objects. IV. Asteroid (1566) Icarus. *Astron. J.* **75**, 186-195.
- Goldstein, R. M. (1968) Radar observations of Icarus. *Science* **162**, 903-904.
- Goldstein, R. M. (1969) Radar observations of Icarus. *Icarus* **10**, 430-431.

- Hicks, M. D., Fink, U., and Grundy, W. M. (1998) The unusual spectra of 15 near-Earth asteroids and extinct comet candidates. *Icarus* **133**, 69-78.
- IAU (1984) Minor Planets Circular MPC 8665. International Astronomical Union, April 15, 1984.
- Kleiman, L. A. (1968) Ed. Project Icarus. M.I.T. Report No. 13, The M.I.T. Press, Cambridge, Massachusetts, 121 pp.
- Lagerkvist, C. -I, Harris, A. W. and Zappala, V. (1989) Asteroid lightcurve parameters. In *Asteroids II* eds. R. P. Binzel, T. Gehrels, and M. S. Matthews, pp. 1162-1179. Univ. of Arizona Press, Tucson.
- McFadden, L.-A., Tholen, D. J. and Veeder, G. J. (1989) Physical properties of Aten, Apollo and Amor asteroids. In *Asteroids II* eds. R. P. Binzel, T. Gehrels, and M. S. Matthews, pp. 442-467. Univ. of Arizona Press, Tucson.
- Miner, E. and Young, J. (1969) Photometric determination of the rotation period of 1566 Icarus. *Icarus* **10**, 436-440.
- Nature (1967) Icarus in Parliament. *Nature* **216**, 529 (News Item).
- Newsweek (1968) Here comes Icarus. **71**, June 17, p. 74
- New York Times (1967) Monitoring of asteroids urged to warn of impending collisions. Oct. 18, Page 30.
- New York Times (1968) Interplanetary flight program urged for U.S. Aug. 15, Page 17.
- New York Times (1969) 23 scientists ask unmanned probe of outer planets. Aug. 4, Pages 1, 11.
- Ostro, S. J. (1993) Planetary radar astronomy. *Rev. Mod. Phys.* **65**, 1235-1279.
- Ostro, S. J., Campbell, D. B., Chandler, J. F., Hine, A. A., Hudson, R. S., Rosema, K. D., and Shapiro, I. I. (1991a) Asteroid 1986 DA: Radar evidence for a metallic composition. *Science*, **252**, 1399-1404.
- Ostro, S. J., Campbell, D. B., Chandler, J. F., Shapiro, I. I., Hine, A. A., Velez, R., Jurgens, R. F., Rosema, K. D., Winkler, R. and Yeomans, D. K. (1991b) Asteroid radar astrometry. *Astron. J.* **102**, 1490-1502.

- Ostro, S. J., Hudson, R. S., Jurgens, R. F., Rosema, K. D., Winkler, R., Howard, D., Rose, R., Slade, M. A., Yeomans, D. K., Giorgini, J. D., Campbell, D. B., Perillat, P., Chandler, J. F., and Shapiro, I. I. (1995) Radar images of asteroid 4179 Toutatis. *Science* **270**, 80-83.
- Pettengill, G. H., Shapiro, I. I., Ash, M. E., Ingalls, R. P., Rainville, L. P., Smith, W. B. and Stone, M. L. (1969) Radar observations of Icarus. *Icarus* **10**, 432-435.
- Shahid-Salass, B. and Yeomans, D. K. (1994) Relativistic effects on the motion of asteroids and comets. *Astronomical J.* **107**, 1885-1889.
- Steele, D. I., McNaught, R. H., Garradd, G. J., Asher, D. J. and Taylor, A. D. (1997). Near-Earth asteroid 1995 HM: a highly-elongated monolith rotating under tension?. *Planet. Space Sci.* **45**, 1091-1098.
- Tedesco, E. F. (1989) Asteroid magnitudes, UVB colors, and IRAS albedos and diameters. In *Asteroids II* eds. R. P. Binzel, T. Gehrels, and M. S. Matthews, pp. 1090-1138. Univ. of Arizona Press, Tucson.
- Tholen, D. J. (1989) Asteroid taxonomic classifications. In *Asteroids II* eds. R. P. Binzel, T. Gehrels, and M. S. Matthews, pp. 1139-1150. Univ. of Arizona Press, Tucson.
- Veeder, G. J., Hanner, M. S., Matson, D. L., Tedesco, E. F., Lebofsky, L. A. and Tokunaga, A. T. (1989) Radiometry of near-earth asteroids. *Astron. J.* **97**, 1211-1219.
- Veverka, J. and Liller, W. (1969) Observations of Icarus: 1968. *Icarus* **10**, 441-444.
- Zellner, B., (1979) Asteroid taxonomy and the distribution of the compositional types. In *Asteroids* ed. T. Gehrels, pp. 783-806. Univ. of Arizona Press, Tucson.

Figure Captions

Fig. 1 Relative rotational phase coverage. Each radial line shows the rotational position of the asteroid at the start of the reception for a particular run, and its length is proportional to the standard deviation of the received signal. The first run (11:58 on 1996/06/08) is arbitrarily taken to be at zero phase (along the arrow), and phase increases clockwise. Thin circles separate the runs for June 8 (innermost), 9, and 10.

Fig. 2 The sum of all 124 single-run spectra, plotted in terms of noise standard deviation: (a) raw spectra, (b) spectra smoothed with a 10-Hz filter, (c) folded and smoothed spectra, and (d) the central portion of (c).

Fig. 3 Chi-square (i.e. the sum of squared residuals) from fitting the spectral model function of Eq. (2) to the OC sum spectrum of Fig. 2a, shown as function of extremal bandwidth and spectral shape parameter of the model function. Note the oblique trough-like minimum.

Fig. 4 Radar albedo (dark solid curve) of Icarus as a function of its effective diameter, calculated with our estimated radar cross-section $\sigma_{OC} = 0.05 \text{ km}^2$. This curve is bounded by thin solid lines representing the $\pm 35\%$ uncertainty. The average radar albedos of representative asteroid types and classes are superimposed on the radar albedo curve. The visual geometric albedo is also plotted (dash-dot line), based on (a) $H = 15.95$ and (b) $H = 16.9$. The asterisks and their accompanying thick solid curve segments represent, respectively, the mean and rms dispersion of the visual geometric albedos for the marked taxonomic classes (Tedesco, 1989).

TABLE I

Selected Articles on Icarus' Earth Approach in 1968

Title	Publication Details
Interplanetary flight program urged for U.S.	<i>New York Times</i> , Aug 15, 1968., P. 17
Monitoring of asteroids urged to warn of impending collisions	<i>New York Times</i> , Oct 18, 1967, p. 30
Hippies flee to Colorado as Icarus nears Earth	<i>New York Times</i> , June 14, 1968, p. 22
Photographs taken of nearing asteroid	<i>New York Times</i> , June 13, 1968, p. 37
23 scientists ask unmanned probe of outer planets	<i>New York Times</i> , Aug. 4, 1969, p. 1, 11
Prediction of Earth-asteroid collision is scouted	<i>New York Times</i> , July 31 1966, p. 54
The threat of the wandering asteroids	<i>New York Times</i> , June 9 1968, p. 12
Despite cultists, Icarus passes by	<i>New York Times</i> , June 15 1968, p. 39
Astronomers take aim as asteroid nears the Earth	<i>New York Times</i> , June 7 1968, p. 41
Data indicate asteroid Icarus may be a sphere of solid iron	<i>New York Times</i> , June 27, 1968, p. 43
Here comes Icarus	<i>Newsweek</i> 71, June 17, 1968, p. 74
Whoosh!	<i>Newsweek</i> 71, June 24, 1968, p.74
Icarus in Parliament	<i>Nature</i> 216, 1967, p. 529
Icarus passes by	<i>Nature</i> 218, 1968, p. 914
Asteroid Icarus flies by the Earth	<i>Sky and Telescope</i> 35, 1968, pp. 345, 408
Icarus flies past the Earth	<i>Sky and Telescope</i> 36, Aug 1968, pp. 75-77
The nature of Icarus	<i>Sky and Telescope</i> 37, Feb 1969, pp. 93-94
Radar echoes from Icarus are received by MIT facility	<i>IEEE Spectrum</i> 5, 1968, p. 130
Radar shows Icarus to be tiny, rough	<i>IEEE Spectrum</i> 6, 1969, p. 16
Duck, here comes Icarus!	<i>Science Digest</i> 62, Oct 1967, p.33
Can a filmed disaster surpass Earth's peril from space? Icarus	<i>Science Digest</i> 85, June 1979, pp. 11-13
Here comes Icarus	<i>Science Digest</i> 63, June 1968, pp. 8-14
Icarus, strange swinger	<i>Science News</i> 92, Nov 18, 1967, p. 490
Photographs of Icarus	<i>Spaceflight</i> 10, 1968, p. 388
Diameter of Icarus believed 900 meters	<i>Aviation Week & Space Tech.</i> 90, Jan 6 1969, p. 77
JPL radar indicates Icarus tiny, very rough	<i>Rev. Pop. Astron.</i> 63, Feb. 1969, p. 32
Avoiding an asteroid: when MIT took on Icarus	<i>Technology Review</i> 88, July 1985, p. 69
Investigation of the motion of the unusual minor planet Icarus	<i>Inst. Theo. Astro.</i> 15, 1984, p. 347
Project Icarus: a book review	<i>Icarus</i> 10, 1969, p. 447
Radar observations of Icarus	<i>Science</i> 162, 1968, p. 903

TABLE II

A Priori Information about Icarus^a

Parameter/Characteristic	Value/Type	Unit	Reference
Semi-major axis	1.078	AU	JPL Database ^b
Eccentricity	0.827		JPL Database ^b
Inclination of orbit ^c	22.870	Degrees	JPL Database ^b
Orbital period	1.12	Years	JPL Database ^b
Taxonomic class	S		Chapman <i>et al.</i> (1975)
	Q		Hicks <i>et al.</i> (1998)
Visual absolute magnitude	15.95	Magnitudes	Tedesco (1989)
	16.4	Magnitudes	JPL Database ^b , Chapman <i>et al.</i> (1994)
	16.9	Magnitudes	IAU (1984)
Maximum light-curve amplitude	0.22	Magnitudes	Lagerkvist <i>et al.</i> (1989)
Rotation period	2.273	Hours	Lagerkvist <i>et al.</i> (1989)
			Gehrels <i>et al.</i> (1970)
			Veverka and Liller (1969)
Visual albedo (Standard model)	0.42		Veeder <i>et al.</i> (1989)
Visual albedo (Rotating model)	0.39		Veeder <i>et al.</i> (1989)

^a Multiple entries for a single parameter or characteristic signify alternative values taken from quoted sources.

^b <http://ssd.jpl.nasa.gov/cgi-bin/et>, <http://ssd.jpl.nasa.gov/cgi-bin/eph> *OK*

^c with reference to J2000 ecliptic

TABLE III

Parameters of CW Radar Data Collection

Date (June '96)	Receive Interval (UTC)	RTT, Sec.	No. of Data Runs
08	11:58 - 15:52	109	43
09	13:08 - 14:57	104	27
10	11:52 - 15:14	101	54

<p><u>Common Parameters</u></p> <p>Radar Frequency (f) = 8510 MHz</p> <p>Wavelength (λ) = 3.5 cm</p> <p>Transmitted Polarization: RCP</p> <p>Received Polarization: Simultaneous OC and SC</p> <p>Basic Processing: 256-point FFT</p> <p>Doppler Frequency Resolution = 1.953 Hz</p>
<p><u>Abbreviations</u></p> <p>RTT: Round Trip Time</p> <p>RCP: Right Circular Polarization</p> <p>OC: Opposite Circular Polarization</p> <p>SC: Same Circular Polarization</p>

TABLE IV

Polarization Behavior of Icarus for Various Bandwidths^a

Doppler Band- width	Lower Bound on Diameter, km	OC Cross Section (σ_{OC}), km ²	SC Cross Section (σ_{SC}), km ²	Polarization Ratio (μ_c) (SC/OC)	OC Albedo	Total (OC+SC) Albedo
15	0.34	0.038±0.005	0.014±0.003	0.377±0.121	0.412	0.567
20	0.46	0.045±0.006	0.015±0.002	0.335±0.097	0.271	0.304
25	0.57	0.045±0.006	0.021±0.003	0.464±0.130	0.173	0.253
30	0.69	0.052±0.006	0.023±0.003	0.441±0.118	0.139	0.200
35	0.80	0.052±0.006	0.027±0.004	0.518±0.133	0.103	0.157
40	0.92	0.053±0.006	0.030±0.004	0.573±0.145	0.079	0.125
45	1.03	0.054±0.006	0.033±0.004	0.624±0.155	0.064	0.104
50	1.15	0.051±0.006	0.036±0.005	0.714±0.172	0.049	0.084
55	1.26	0.050±0.006	0.038±0.005	0.756±0.182	0.040	0.070
60	1.38	0.050±0.006	0.034±0.004	0.681±0.161	0.033	0.056

^a The uncertainties quoted herein reflect the variances due to the statistical nature of the signal, and do not reflect the radar calibration errors, which raise the fractional uncertainty to ~35%.

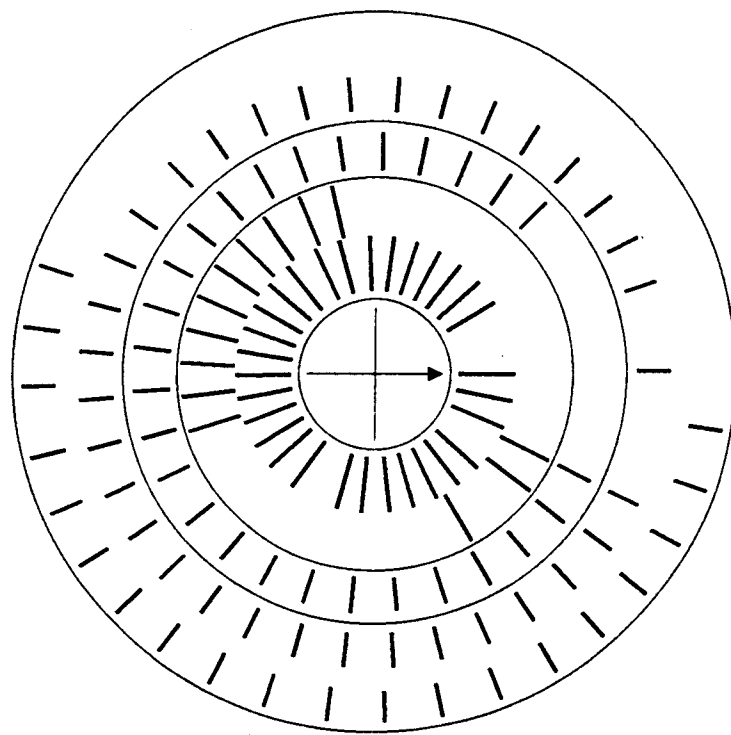


Fig. 1

3-DAY SUM SPECTRA

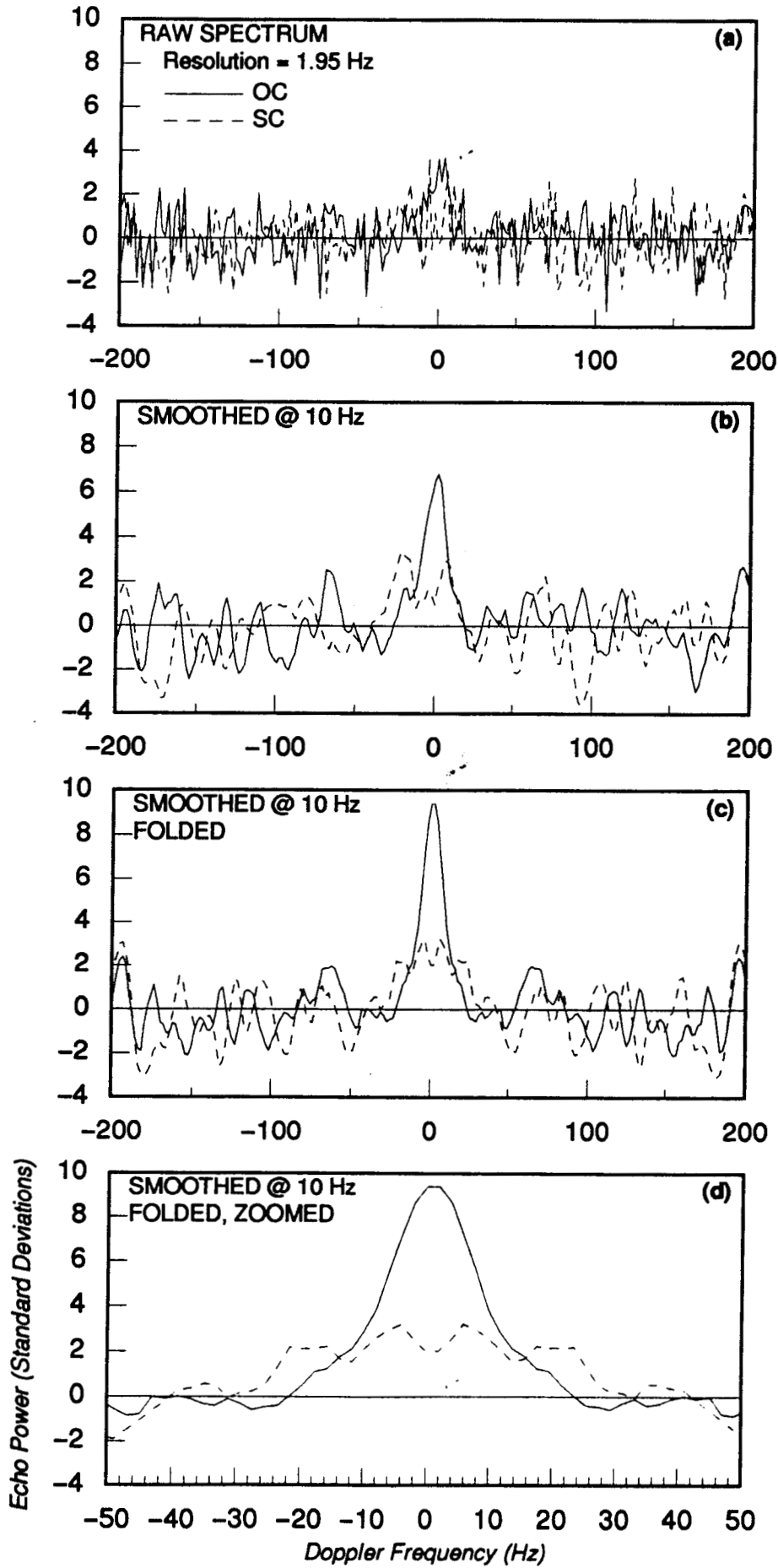


Fig. 2

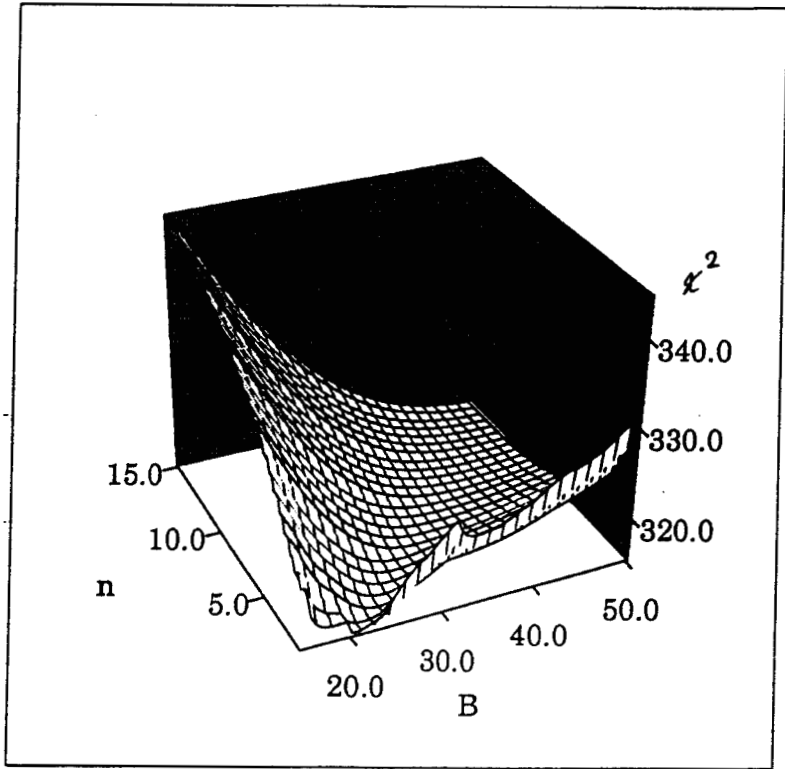


Fig. 3

Fig. 4

